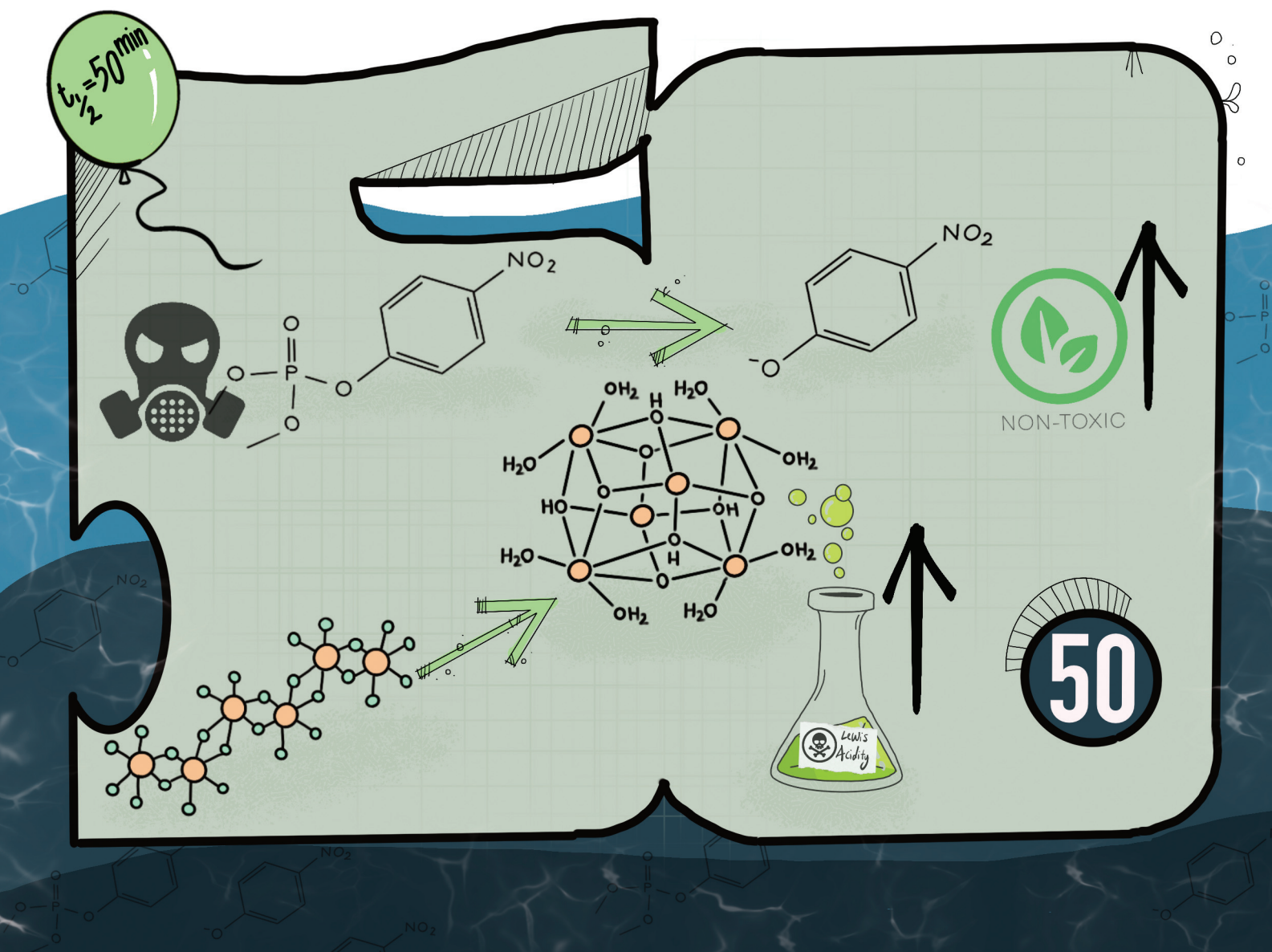


Dalton Transactions

An international journal of inorganic chemistry

rsc.li/dalton



ISSN 1477-9226

COMMUNICATION

[View Article Online](#)
[View Journal](#) | [View Issue](#)

Cite this: *Dalton Trans.*, 2021, **50**, 3116

Received 19th January 2021,
Accepted 1st February 2021

DOI: 10.1039/d1dt00180a

rsc.li/dalton

Tuning the Lewis acidity of metal–organic frameworks for enhanced catalysis†

Venkata Swaroopa Datta Devulapalli,^a Méli ssandre Richard,^a Tian-Yi Luo,^b Mattheus L. De Souza,^b Nathaniel L. Rosi^b and Eric Borguet^b      

The kinetics of hydrolysis of dimethyl nitrophenyl phosphate (DMNP), a simulant of the nerve agent Soman, was studied and revealed transition metal salts as catalysts. The relative rates of DMNP hydrolysis by zirconium and hafnium chlorides are in accordance with their Lewis acidity. *In situ* conversion of zirconium chloride to zirconium oxy-hydroxide was identified as the key step. We propose a precursor-MOF activity relationship.

The development of materials which can detect, adsorb and readily degrade toxic chemicals such as chemical warfare agents (CWAs) is essential to mitigate their harmful effects on military and civilians. CWAs include a wide range of chemicals with a variety of functional groups. They are broadly classified as nerve agents (organophosphorus molecules), vesicants (mustards and arsenicals), blood agents (cyanide containing molecules) and choking agents (phosgene and derivatives).¹ Out of these, organophosphorus nerve agents are lethal considering their immediate and severe impact on the nervous system, thereby affecting simple life processes, leading to death in a short time.² Small amounts of these nerve agents used in the form of aerosol, gas, liquid or adsorbed on solids cause serious long-term effects.

It is clear that a better understanding of the mechanisms of action of materials that can readily adsorb and efficiently degrade these toxic chemicals is crucial to find the best formulation. Early studies of nerve agent detoxification utilized oxides of transition metals such as zirconium oxides,³ hydroxides⁴ or titanium oxides.⁵ Oxides dispersed in polymers were also studied for the oxidation of sulfur mustards.⁶ One major disadvantage of these materials was the low surface areas, low porosity and active site poisoning after nerve agent sorption

resulting in low efficiency of the catalyst.⁷ Other studies report the sorption of dimethyl methyl phosphonate (DMMP) and its photocatalytic degradation by TiO₂ using UV light⁵ which may be challenging for in-operando applications. Thus, different techniques and new materials have been explored for efficient and targeted CWA degradation. Metal–organic frameworks (MOFs) are crystalline organic porous materials with high surface areas and porosities.⁸ MOFs consist of inorganic metal/metal oxide (and/or hydroxide) clusters linked together in 3 dimensions by organic molecules (linkers) *via* coordination bonding. The high degree of property tunability using simple chemistry such as modification of the linkers is one of the attractive features of MOFs. The freedom of choosing the metal/metal cluster, and also the organic linker, facilitates the generation of MOFs with a myriad of topologies, suitable for separations and catalysis.^{9,10} Moreover, the facile functionalization of MOFs makes them appropriate for targeted applications in the fields of gas sorption and bio-medical applications.^{11–14}

Zirconium MOFs have been explored for their ability to catalyze several reactions. Different techniques such as UV-vis,¹⁵ *in situ* FTIR,¹⁶ *in situ* X-ray,¹⁷ TPD,^{16,18} DRIFTS,¹⁷ NMR¹⁹ and also theoretical modelling^{17,20} have been utilized to study the interactions between the molecules and MOFs. Particularly, for the hydrolysis of organophosphorus nerve agents such as Sarin (GB), Soman (GD) and nerve agent simulants, zirconium MOFs have proven to be efficient catalysts. Reports suggest that zirconium MOFs were chosen not only due to the similarities in chemistry with their hydroxides which degrade CWA simulants, but also because they mimic the structure of phosphotriesterase enzyme,²¹ present in nature, that can catalytically hydrolyze the P–O bond of phosphate/phosphonate containing molecules. Hence many zirconium MOFs such as UiO MOFs,²² NU-1000,¹⁵ MOF-808²³ were tested for organophosphorus nerve agent detoxification under basic conditions (buffer pH = 8–10) where the nucleophilic cleavage of P–O is favored, and Zr⁴⁺ shows a strong Lewis acidity character. Additionally, recent studies have focused on CWA degradation

^aDepartment of Chemistry, Temple University, Philadelphia, Pennsylvania 19122, USA. E-mail: eborguet@temple.edu

^bDepartment of Chemistry, University of Pittsburgh, Pittsburgh, Pennsylvania 15261, USA

†Electronic supplementary information (ESI) available. See DOI: 10.1039/d1dt00180a

by MOFs in neutral pH,²⁴ under the effects of ambient gases²⁵ and using polymers such as polyethyleneimine (PEI), which are crucial for practical applications.²⁶ Moreover, defects in MOFs play a decisive role in catalysis and destruction of CWAs. For instance, theoretical and experimental studies performed under UHV, showed that the initial binding and the degradation of live agent/simulant on MOFs surface requires a Lewis-acidic under-coordinated (defect) zirconium site.^{18,27} It was observed that UiO-67 zirconium MOFs were able to degrade DMMP,¹⁸ whereas similar studies performed by Ruffley *et al.* using nearly pristine, defect free UiO-67 MOFs revealed simple physisorption without any degradation.¹⁶

As for all catalytic reactions, a clearer understanding of the role of the catalyst and the nature of active species responsible is necessary for an optimal catalyst selection and better reaction kinetics. However, the effect of MOF precursors on CWA hydrolysis (*e.g.* DMNP hydrolysis) is seldom discussed. We believe that the fundamental properties of MOFs, especially chemical, are best represented and governed by their precursors. Hence, we expect that, a critical understanding of the reactivity of a MOF, in a particular reaction, can be achieved *via* an analysis of the MOF's constituents. Moreover, predicting their properties by testing the precursors could motivate the effort of MOF synthesis and provide a direct way of comparing different MOFs for a particular reaction, in a short time, without actually synthesizing them.

As CWAs are lethal and working with them requires great caution and specialized personal protective equipment, our study was carried out using simulants, *i.e.*, molecules that are structurally and/or chemically similar to nerve agents but relatively less toxic. We investigated the roles of the UiO-67 MOF precursors, zirconium chloride (ZrCl_4), nanoparticulate zirconium hydroxide (Zr(OH)_4) and the biphenyl dicarboxylic acid (BPDC) linker, in dimethyl nitrophenyl phosphate (DMNP) hydrolysis under basic conditions as shown in Fig. 1. DMNP was chosen as a simulant of the nerve agent Soman (GD) for its similarities in structure and heat of adsorption, based on the study performed by Agrawal *et al.*²⁸

Under basic conditions (pH = 10), DMNP hydrolysis leads to the formation of 4-nitrophenolate and dimethyl hydrogen phosphate as products (Fig. 1). The dark yellow 4-nitrophenolate has an absorption band that peaks at ~ 400 nm whose intensity is monitored with time to follow the reaction progress. The addition of DMNP to the buffer solution containing UiO-67 MOFs leads to the catalytic degradation of DMNP with a half-life of ~ 10 min (Fig. 2). In the absence of the MOF little

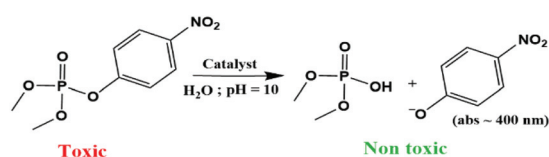


Fig. 1 Hydrolysis of DMNP, simulant of the nerve agent Soman (GD), using a catalyst under basic buffer conditions.

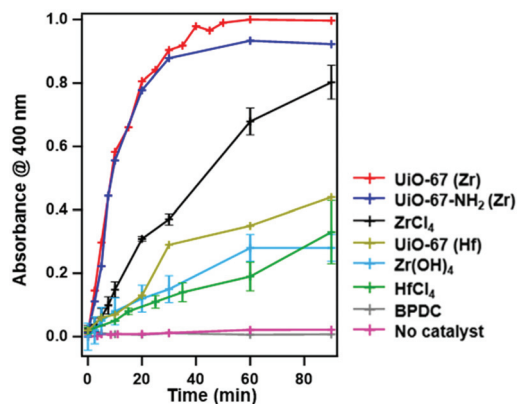


Fig. 2 Progress of DMNP hydrolysis catalyzed by UiO-67 MOFs and their precursors monitored by the formation of 4-nitrophenolate using UV-vis spectroscopy.

change in absorbance after 90 min is observed showing that the reaction does not proceed if it is not catalyzed. In addition, substitution of the MOF linker with NH_2 group on the *meta* position of the benzene ring does not impact the initial rate of the reaction significantly, (Fig. 2) and $\sim 90\%$ overall DMNP conversion for UiO-67- NH_2 vs. $\sim 100\%$ conversion for UiO-67 is observed.

Interestingly, we noticed that the precursor of the UiO-67 MOF nodes, ZrCl_4 , was able to hydrolyze DMNP but with a slower rate ($\sim 65\%$ conversion after 60 min) compared to that of MOFs. However, similar experiments using the linker (BPDC) showed no hydrolysis activity towards DMNP. Based on the obtained results, other precursors of MOFs were tested. Our observations highlight that nanoparticulate Zr(OH)_4 was also active for the degradation of DMNP. However, Zr(OH)_4 shows slower kinetics ($\sim 40\%$ conversion after 60 min) than ZrCl_4 and seems to reach a maximum DMNP conversion at an absorbance of 0.4 after 60 min of reaction.

Previous studies performed by Mondloch *et al.* concluded that bulk Zr(OH)_4 cannot catalyze DMNP hydrolysis.¹⁵ Our study reveals that nanoparticulate Zr(OH)_4 can degrade DMNP, in agreement with studies revealing the activity of Zr(OH)_4 to degrade the nerve agent GD itself.²⁹ The enhanced catalytic activity of the nanoparticles may be attributed to their higher active surface area, and increased number of defects, as well as differences in morphology and electronic structure compared to that of bulk. This result suggests that zirconium metal precursors would be the origin for the activity of zirconium MOFs and attests that at least one of the precursors of the MOF should catalyze the degradation in order for the MOF itself to do the same. As seen in Fig. 2, linker substitution on the *meta* position does not have a significant impact on the rate of DMNP hydrolysis, contrary to previous reports where enhancement in rate of hydrolysis of DMNP was observed using *ortho* and *meta*-amine substituted zirconium MOFs.³⁰ A plausible explanation for the differences in rates of hydrolysis could be the concentration of defects in the MOF resulting from differences in the synthesis procedures.

Hydrolysis of organophosphorus molecules by MOFs is reported to occur *via* nucleophilic attack on P–X bond on live agents (P–O in DMNP) by the available free hydroxyl groups on the node of the UiO MOFs.²⁰ In addition to the accessibility, the nucleophilicity of free hydroxyl groups is directly proportional to the Lewis acidity of the metal they are bound to. When the same reaction is performed with ZrCl_4 the rate of hydrolysis is reduced with $t_{1/2}$ being approximately 50 min (Table S11†). Astle *et al.* reported *in situ* conversion of ZrCl_4 to an active zirconium oxy-hydroxide, which resembles the node of the MOF containing oxy, hydroxyl and aquo groups.³¹ We believe that this oxy-hydroxide can serve as a catalyst for the decomposition of the nerve agent and its simulants. The experiments reported here, in agreement with a previous study,²⁹ suggest that the active site of the MOF, responsible for DMNP hydrolysis, is the inorganic zirconium node.

Compared to Zr(OH)_4 , ZrCl_4 has higher activity for the degradation of DMNP, which can be attributed to higher solubility observed in water of ZrCl_4 compared to Zr(OH)_4 . The labile chlorine ions are reported to favor the hydrolysis of ZrCl_4 , forming ZrOCl_2 , which is further hydrolyzed to form zirconium oxy-hydroxide.³²

The zirconium oxy-hydroxide formed in the solution exhibits a high degree of similarity to the MOF node, as depicted in Fig. 3, thus displaying activities comparable to MOFs. This hydrolysis is less likely in the case of Zr(OH)_4 thereby resulting in lower activity of Zr(OH)_4 .³¹ In fact, the non-zero background of Zr(OH)_4 (corrected in Fig. 2) suggests scattering by undissolved Zr(OH)_4 particles. However, no background absorbance was observed for UiO-67 MOF or ZrCl_4 suggesting smaller crystallites compared to Zr(OH)_4 (Fig. S11–3†).

Interestingly, a study performed on UiO-66, by Bůžek *et al.*, reports that the widely employed reaction conditions (pH = 10) to test nerve agent degradation/simulant degradation destabilizes the MOF *via* breakage of Zr–OC bond between the metal node and the linker, thereby allowing the active node material

to leach into the solution and catalyze the reaction.³³ Based on this study, it is reasonable to expect that mechanistically, ZrCl_4 also behaves in similar fashion to MOFs in the hydrolysis of DMNP (dissolution followed by generation of catalytic species).

Utilizing the insights from theoretical studies on nerve agent degradation by MOFs,^{20,34} a base catalyzed hydrolysis mechanism of DMNP degradation by *in situ* formed zirconium oxy-hydroxide is presented in Fig. 4. Step i represents association of DMNP and H_2O to the Zr in the node. Subsequently in step ii, nucleophilic attack by oxygen on the electrophilic P=O results in the release of 4-nitrophenolate and dimethyl hydrogen phosphate as products (steps iii and iv).

Previous literature reports, and the results obtained from our studies, have motivated us to formulate a relationship between the activity of MOFs and the activity of their precursors. Hence, we hypothesize that at least one of the MOF precursors should be active in hydrolyzing DMNP, under basic conditions, and that Lewis acidity of the metal node plays a determinant role in this activity. To validate our hypothesis, the effect of a different metal MOF, *i.e.* UiO-67(Hf) and its precursor hafnium chloride (HfCl_4) were tested to evaluate their efficiency towards the hydrolysis of DMNP.

The choice of hafnium was motivated by the fact that this element belongs to the same group as zirconium. The interesting difference is that hafnium is relatively less Lewis acidic than zirconium.³⁵ As expected HfCl_4 displayed lower activity towards DMNP hydrolysis in basic medium compared to ZrCl_4 (Fig. 2), confirming the crucial role of Lewis acidity in this reaction. According to our proposed hypothesis, one would expect a lower activity of UiO-67(Hf) towards DMNP hydrolysis and indeed, UiO-67 (Hf) displayed lower activity compared to UiO-67 (Zr). This observation clearly validates our precursor-MOF hypothesis – the higher the activity of the MOF precursor for DMNP degradation, higher will be the activity of the MOF itself. In a computational study performed by Mendonca *et al.*, the effects of the metal node, its topology and connectivity on the hydrolysis of 6 nerve agents were systematically studied and zirconium MOFs performed better than hafnium MOFs

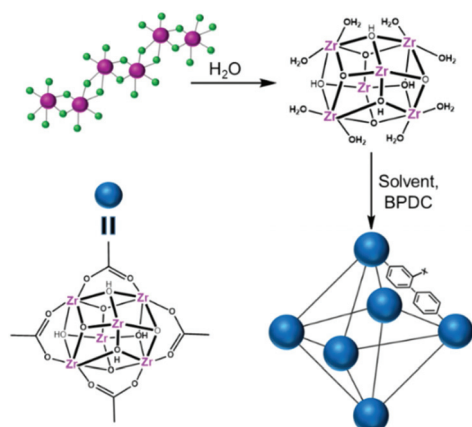


Fig. 3 Hydrolysis of zirconium chloride to form zirconium oxyhydroxide, which can coordinatively interact with linkers (BPDC) in the presence of a solvent to form the MOF. Pink, green, and blue spheres represent zirconium, chlorine and the MOF node, respectively.

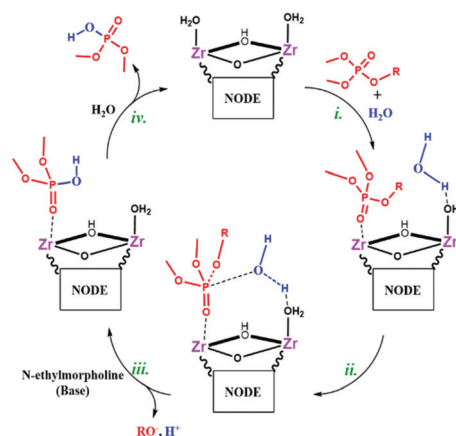


Fig. 4 Mechanism of base catalyzed hydrolysis of DMNP by zirconium oxy-hydroxide (in figure, R: 4-nitrophenyl).

irrespective of the nerve agent/MOF identity,³⁶ which is in line with our verified hypothesis and predictions.

In a recent study by Lionetti *et al.*, the qualitative rate of oxygen atom transfer (OAT) in heterometallic cubanes was observed to increase with increasing Lewis acidity of the redox inactive metal, thus providing a handle to tune the OAT reactivity of the cubane clusters.³⁷ Another study performed by Johnson *et al.* on cobalt assisted Fischer–Tropsch synthesis reports a positive correlation between the Lewis acidity of the metal oxide promoter, product selectivity and the rate coefficient, thereby establishing a guideline for a rational selection of promoter materials.³⁸ Therefore, the paradigm proposed in this paper of using the MOF precursors as models to predict the activity of the MOF itself should guide researchers in clearly and rapidly choosing the optimum metals for synthesizing suitable MOFs for DMNP hydrolysis or any other specific reaction.

In summary, the efficiency of zirconium MOFs and their precursors for the hydrolysis of DMNP, in a basic buffer medium, was investigated. Our results support the fact that the active site in UiO-67 MOFs responsible for the hydrolysis of DMNP is the metal node and is dependent on the Lewis-acidic strength of the metal. Due to a higher solubility of ZrCl_4 (which favors formation of zirconium oxy-hydroxide) compared to $\text{Zr}(\text{OH})_4$, the rate of hydrolysis of DMNP by ZrCl_4 was higher compared to $\text{Zr}(\text{OH})_4$. No DMNP hydrolysis was observed due to the BPDC linker. This suggests that at least one of the precursors has to be active in order for the MOF to hydrolyze DMNP. Based on our results we hypothesized that MOFs made with precursors showing high activity for a reaction will in turn exhibit higher activity for the same reaction. Tests performed using UiO-67(Hf) and HfCl_4 revealed a slower rate of DMNP hydrolysis compared to UiO-67(Zr) and ZrCl_4 respectively, in line with the lower Lewis acidities of the Hf based materials, thus validating our hypothesis. We expect that our precursor-MOF activity hypothesis will guide in choosing the right metal, based on its Lewis acidity, for synthesizing MOFs that can actively destroy DMNP and relevant organophosphorus nerve agents/their simulants, as well as for catalyzing other organic reactions.

Conflicts of interest

There are no conflicts to declare.

Acknowledgements

This project received support from the Defense Threat Reduction Agency (DTRA) (grant no. HDTRA1-16-1-0044). M. L. D. acknowledges support from the University of Pittsburgh through a Dietrich School of Arts and Sciences graduate research fellowship. This work was performed, in part, at the Nanoscale Fabrication and Characterization Facility, a laboratory of the Gertrude E. and John M. Petersen

Institute of NanoScience and Engineering, housed at the University of Pittsburgh. VSDD and EB thank Dr Ramanathan Vaidhyathan from the Indian Institute of Science Education and Research, Pune, India for useful discussions.

Notes and references

- 1 K. Ganesan, S. Raza and R. Vijayaraghavan, *J. Pharm. BioAllied Sci.*, 2010, **2**, 166–178.
- 2 M. B. Colovic, D. Z. Krstic, T. D. Lazarevic-Pasti, A. M. Bondzic and V. M. Vasic, *Curr. Neuropharmacol.*, 2013, **11**, 315–335.
- 3 V. V. Singh, A. Martin, K. Kaufmann, S. D. S. de Oliveira and J. Wang, *Chem. Mater.*, 2015, **27**, 8162–8169.
- 4 S. Kim, W. B. Ying, H. Jung, S. G. Ryu, B. Lee and K. J. Lee, *Chem. – Asian J.*, 2017, **12**, 698–705.
- 5 C. N. Rusu and J. T. Yates, *J. Phys. Chem. B*, 2000, **104**, 12299–12305.
- 6 J. Henych, V. Stengl, A. Mattsson, J. Tolasz and L. Osterlund, *J. Hazard. Mater.*, 2018, **359**, 482–490.
- 7 D. A. Panayotov and J. R. Morris, *Langmuir*, 2009, **25**, 3652–3658.
- 8 M. Eddaoudi, J. Kim, N. Rosi, D. Vodak, J. Wachter, M. O’Keeffe and O. M. Yaghi, *Science*, 2002, **295**, 469–472.
- 9 A. H. Assen, Y. Belmabkhout, K. Adil, P. M. Bhatt, D. X. Xue, H. Jiang and M. Eddaoudi, *Angew. Chem., Int. Ed.*, 2015, **54**, 14353–14358.
- 10 F. J. Song, C. Wang and W. B. Lin, *Chem. Commun.*, 2011, **47**, 8256–8258.
- 11 Y. C. Ma, Y. H. Zhu, X. F. Tang, L. F. Hang, W. Jiang, M. Li, M. I. Khan, Y. Z. You and Y. C. Wang, *Biomater. Sci.*, 2019, **7**, 2740–2748.
- 12 K. D. Lu, C. B. He and W. B. Lin, *J. Am. Chem. Soc.*, 2014, **136**, 16712–16715.
- 13 Q. Guan, Y. A. Li, W. Y. Li and Y. B. Dong, *Chem. – Asian J.*, 2018, **13**, 3122–3149.
- 14 G. X. Lan, K. Y. Ni, S. S. Veroneau, X. Y. Feng, G. T. Nash, T. K. Luo, Z. W. Xu and W. B. Lin, *J. Am. Chem. Soc.*, 2019, **141**, 4204–4208.
- 15 J. E. Mondloch, M. J. Katz, W. C. Isley, P. Ghosh, P. L. Liao, W. Bury, G. Wagner, M. G. Hall, J. B. DeCoste, G. W. Peterson, R. Q. Snurr, C. J. Cramer, J. T. Hupp and O. K. Farha, *Nat. Mater.*, 2015, **14**, 512–516.
- 16 J. P. Ruffley, I. Goodenough, T. Y. Luo, M. Richard, E. Borguet, N. L. Rosi and J. K. Johnson, *J. Phys. Chem. C*, 2019, **123**, 19748–19758.
- 17 A. M. Plonka, Q. Wang, W. O. Gordon, A. Balboa, D. Troya, W. W. Guo, C. H. Sharp, S. D. Senanayake, J. R. Morris, C. L. Hill and A. I. Frenkel, *J. Am. Chem. Soc.*, 2017, **139**, 599–602.
- 18 G. Wang, C. Sharp, A. M. Plonka, Q. Wang, A. I. Frenkel, W. Guo, C. Hill, C. Smith, J. Kollar, D. Troya and J. R. Morris, *J. Phys. Chem. C*, 2017, **121**, 11261–11272.
- 19 M. C. de Koning, G. W. Peterson, M. van Grol, I. Iordanov and M. McEntee, *Chem. Mater.*, 2019, **31**, 7417–7424.

- 20 D. Troya, *J. Phys. Chem. C*, 2016, **120**, 29312–29323.
- 21 M. J. Katz, J. E. Mondloch, R. K. Totten, J. K. Park, S. T. Nguyen, O. K. Farha and J. T. Hupp, *Angew. Chem., Int. Ed.*, 2014, **53**, 497–501.
- 22 M. Kalaj, J. M. Palomba, K. C. Bentz and S. M. Cohen, *Chem. Commun.*, 2019, **55**, 5367–5370.
- 23 S. Y. Moon, Y. Y. Liu, J. T. Hupp and O. K. Farha, *Angew. Chem., Int. Ed.*, 2015, **54**, 6795–6799.
- 24 S. J. Garibay, O. K. Farha and J. B. DeCoste, *Chem. Commun.*, 2019, **55**, 7005–7008.
- 25 H. Wang, J. J. Mahle, T. M. Tovar, G. W. Peterson, M. G. Hall, J. B. DeCoste, J. H. Buchanan and C. J. Karwacki, *ACS Appl. Mater. Interfaces*, 2019, **11**, 21109–21116.
- 26 Z. J. Chen, T. Islamoglu and O. K. Farha, *ACS Appl. Nano Mater.*, 2019, **2**, 1005–1008.
- 27 J. A. Harvey, M. L. McEntee, S. J. Garibay, E. M. Durke, J. B. DeCoste, J. A. Greathouse and D. F. S. Gallis, *J. Phys. Chem. Lett.*, 2019, **10**, 5142–5147.
- 28 M. Agrawal, D. F. S. Gallis, J. A. Greathouse and D. S. Sholl, *J. Phys. Chem. C*, 2018, **122**, 26061–26069.
- 29 T. J. Bandosz, M. Laskoski, J. Mahle, G. Mogilevsky, G. W. Peterson, J. A. Rossin and G. W. Wagner, *J. Phys. Chem. C*, 2012, **116**, 11606–11614.
- 30 T. Islamoglu, M. A. Ortuno, E. Proussaloglou, A. J. Howarth, N. A. Vermeulen, A. Atilgan, A. M. Asiri, C. J. Cramer and O. K. Farha, *Angew. Chem., Int. Ed.*, 2018, **57**, 1949–1953.
- 31 M. A. Astle, G. A. Rance, M. W. Fay, S. Notman, M. R. Sambrook and A. N. Khlobystov, *J. Mater. Chem. A*, 2018, **6**, 20444–20453.
- 32 F. P. Venable, *J. Elisha Mitchell Sci. Soc.*, 1920, **36**, 115–122.
- 33 D. Bůžek, J. Demel and K. Lang, *Inorg. Chem.*, 2018, **57**, 14290–14297.
- 34 K. O. Kirlikovali, Z. J. Chen, T. Islamoglu, J. T. Hupp and O. K. Farha, *ACS Appl. Mater. Interfaces*, 2020, **12**, 14702–14720.
- 35 J. F. Lyu, X. Zhang, P. Li, X. J. Wang, C. T. Buru, P. Bai, X. H. Guo and O. K. Farha, *Chem. Mater.*, 2019, **31**, 4166–4172.
- 36 M. L. Mendonca, D. Ray, C. J. Cramer and R. Q. Snurr, *ACS Appl. Mater. Interfaces*, 2020, **12**, 35657–35675.
- 37 D. Lionetti, S. Suseno, E. Y. Tsui, L. Lu, T. A. Stich, K. M. Carsch, R. J. Nielsen, W. A. Goddard, R. D. Britt and T. Agapie, *Inorg. Chem.*, 2019, **58**, 2336–2345.
- 38 G. R. Johnson and A. T. Bell, *J. Catal.*, 2016, **338**, 250–264.